

MIT Open Access Articles

*Observation of $B[0 \text{ over } s] \rightarrow [\text{bar over } D][\text{superscript } 0]K[0 \text{ over } S]$ and Evidence for $B[0 \text{ over } s] \rightarrow [\text{bar over } D][\text{superscript } *0]K[0 \text{ over } S]$ Decays*

The MIT Faculty has made this article openly available. **Please share** how this access benefits you. Your story matters.

Citation: Aaij, R., C. Abellan Beteta, B. Adeva, M. Adinolfi, A. Affolder, Z. Ajaltouni, S. Akar, et al. "Observation of $B[0 \text{ over } s] \rightarrow [\text{bar over } D][\text{superscript } 0]K[0 \text{ over } S]$ and Evidence for $B[0 \text{ over } s] \rightarrow [\text{bar over } D][\text{superscript } *0]K[0 \text{ over } S]$ Decays." *Physical Review Letters* 116, no. 16 (April 21, 2016). © 2016 CERN, for the LHCb Collaboration

As Published: <http://dx.doi.org/10.1103/PhysRevLett.116.161802>

Publisher: American Physical Society

Persistent URL: <http://hdl.handle.net/1721.1/102299>

Version: Final published version: final published article, as it appeared in a journal, conference proceedings, or other formally published context

Terms of use: Creative Commons Attribution



Observation of $B_s^0 \rightarrow \bar{D}^0 K_S^0$ and Evidence for $B_s^0 \rightarrow \bar{D}^{*0} K_S^0$ Decays

R. Aaij *et al.**

(LHCb Collaboration)

(Received 9 March 2016; published 21 April 2016)

The first observation of the $B_s^0 \rightarrow \bar{D}^0 K_S^0$ decay mode and evidence for the $B_s^0 \rightarrow \bar{D}^{*0} K_S^0$ decay mode are reported. The data sample corresponds to an integrated luminosity of 3.0 fb^{-1} collected in pp collisions by LHCb at center-of-mass energies of 7 and 8 TeV. The branching fractions are measured to be

$$\begin{aligned} \mathcal{B}(B_s^0 \rightarrow \bar{D}^0 \bar{K}^0) &= [4.3 \pm 0.5(\text{stat}) \pm 0.3(\text{syst}) \pm 0.3(\text{frag}) \pm 0.6(\text{norm})] \times 10^{-4}, \\ \mathcal{B}(B_s^0 \rightarrow \bar{D}^{*0} \bar{K}^0) &= [2.8 \pm 1.0(\text{stat}) \pm 0.3(\text{syst}) \pm 0.2(\text{frag}) \pm 0.4(\text{norm})] \times 10^{-4}, \end{aligned}$$

where the uncertainties are due to contributions coming from statistical precision, systematic effects, and the precision of two external inputs, the ratio f_s/f_d and the branching fraction of $B^0 \rightarrow \bar{D}^0 K_S^0$, which is used as a calibration channel.

DOI: [10.1103/PhysRevLett.116.161802](https://doi.org/10.1103/PhysRevLett.116.161802)

The study of CP violation is one of the most important topics in flavor physics. In B^0 decays, the phenomenon of CP violation has been extensively studied at *BABAR*, *Belle*, and LHCb, which confirmed many predictions of the standard model (SM) [1–4]. Nowadays, the focus is on the search for beyond the standard model (BSM) effects by improving the statistical precision of the CP violation parameters and looking for deviations from the SM predictions.

In the SM, violation of CP symmetry in B decays is commonly parametrized by three phase angles (α , β , γ) derived from the Cabibbo-Kobayashi-Maskawa matrix, which describes the charged-current interactions among quarks [5]. Since the angles sum up to 180° , any deviation found in measurements of the phases would be a sign of BSM physics affecting at least one of the results. Currently the angle γ is only known with an uncertainty of about 10° [6]; experimental efforts are required to improve its precision and thus the sensitivity to BSM effects. Another sensitive observable is the B_s^0 mixing phase, ϕ_s , which in the SM is predicted with good precision to be close to zero [7]. Any significant deviation here would also reveal physics BSM [8,9]. The current uncertainty is $O(0.1)$ rad [6].

In this Letter, two decay modes that can improve the knowledge of γ and ϕ_s are studied. The $B^0 \rightarrow \bar{D}^0 K_S^0$ decay [10] offers a determination of the angle γ with small theoretical uncertainties [11], while $B_s^0 \rightarrow \bar{D}^{*0} K_S^0$, similar

to the $B_s^0 \rightarrow \bar{D}^{(*)0} \phi$ [12] mode, provides sensitivity to ϕ_s with a theoretical accuracy of $O(0.01)$ rad [13].

While the decay $B^0 \rightarrow \bar{D}^{(*)0} K_S^0$ has been seen at the B factories [14], $B_s^0 \rightarrow \bar{D}^{(*)0} K_S^0$ decays have not previously been observed. Theoretical predictions of their branching fractions are of the order of 5×10^{-4} [15–17]. This Letter reports the first observation of $B_s^0 \rightarrow \bar{D}^0 K_S^0$ and evidence for $B_s^0 \rightarrow \bar{D}^{*0} K_S^0$ decays, and it provides measurements of branching fractions of these channels normalized to $B^0 \rightarrow \bar{D}^0 K_S^0$ decays.

The analysis is based on data collected in pp collisions by the LHCb experiment at $\sqrt{s} = 7$ and 8 TeV corresponding to an integrated luminosity of 3.0 fb^{-1} . The LHCb detector [18,19] is a single-arm forward spectrometer covering the pseudorapidity range $2 < \eta < 5$, designed for the study of particles containing b or c quarks. The detector includes a high-precision tracking system consisting of a silicon-strip vertex detector surrounding the pp interaction region, a large-area silicon-strip detector located upstream of a dipole magnet with a bending power of about 4 T m, and three stations of silicon-strip detectors and straw drift tubes placed downstream of the magnet. The tracking system provides a measurement of momentum, p , of charged particles with a relative uncertainty that varies from 0.5% at low momentum to 1.0% at 200 GeV/ c . Two ring-imaging Cherenkov (RICH) detectors are able to discriminate between different species of charged hadrons. The online event selection is performed by a trigger, which consists of a hardware stage, based on information from the calorimeter and muon systems, followed by a software stage, which applies a full event reconstruction.

In the simulation, pp collisions are generated using PYTHIA [20] with a specific LHCb configuration [21]. Decays of hadronic particles are described by EVTGEN

*Full author list given at the end of the article.

Published by the American Physical Society under the terms of the Creative Commons Attribution 3.0 License. Further distribution of this work must maintain attribution to the author(s) and the published article's title, journal citation, and DOI.

[22], in which final-state radiation is generated using PHOTOS [23]. The interaction of the generated particles with the detector, and its response, are implemented using the GEANT4 toolkit [24] as described in Ref. [25].

At the hardware trigger stage, events are required to have a muon with high p_T or a hadron, photon, or electron with high transverse energy deposited in the calorimeters. The software trigger requires a two-, three-, or four-track secondary vertex with a significant displacement from any reconstructed primary vertex (PV). At least one of these tracks must have $p_T > 1.7$ GeV/ c and be inconsistent with originating from a PV. A multivariate algorithm [26] is used to identify secondary vertices consistent with the decay of a b hadron.

Candidate $K_S^0 \rightarrow \pi^+\pi^-$ decays are reconstructed in two different categories, the first involving K_S^0 mesons that decay early enough for the daughter pions to be reconstructed in the vertex detector, referred to as *long*, and the second containing K_S^0 's that decay later, such that track segments of the pions cannot be formed in the vertex detector, referred to as *downstream*. The long category has better mass, momentum, and vertex resolution than the downstream category. Long (downstream) K_S^0 candidates are required to have decay lengths larger than 12 (9) times the decay length uncertainty. The invariant mass of the candidate is required to be within 30 MeV/ c^2 of the known K_S^0 mass [27].

The $\bar{D}^0 \rightarrow K^+\pi^-$ candidates are formed from combinations of kaon and pion candidate tracks identified by the RICH detectors. The pion (kaon) must have $p > 1(5)$ GeV/ c and $p_T > 100(500)$ MeV/ c , and it must be inconsistent with originating from a PV. The invariant mass of the candidate is required to be within 50 MeV/ c^2 of the known \bar{D}^0 mass [27].

The B (B^0 or B_s^0) candidate is formed by combining \bar{D}^0 and K_S^0 candidates and requiring an invariant mass in the range 4500–7000 MeV/ c^2 , a decay time greater than 0.2 ps, and a momentum vector pointing back to the associated PV. To improve the mass resolution of the B candidates, a kinematic fit is performed constraining the masses of the \bar{D}^0 and K_S^0 candidates to the known values [27].

The purity of the B candidate sample is then increased by means of a multivariate classifier [28,29] that separates the signal from the combinatorial background. Separate algorithms are trained for candidates with long and downstream K_S^0 candidates. The discriminating variables used in the classifier are the χ^2 of the kinematic fit, geometric variables related to the finite lifetime of the B , \bar{D}^0 , and K_S^0 , the decay time, and the p_T and p of the K_S^0 candidate. The multivariate classifier is trained and tested using signal candidates from simulations and background candidates from data in the upper sideband of the B mass spectrum, corresponding to $m(\bar{D}^0 K_S^0) > 5500$ MeV/ c^2 , where no backgrounds are expected from B decays in which a

photon or a π meson is not reconstructed. The selection is optimized to minimize the statistical uncertainty on the ratio of B_s^0 over B^0 signal event yields. The signal efficiency and background rejection factors are 76% and 98%, respectively. B candidates in the mass range 5000–5900 MeV/ c^2 are retained. Multiple candidates occur in 0.2% (0.4%) of long (downstream) K_S^0 events, in which case one candidate, chosen at random, is kept.

The B_s^0 and B^0 signal yields in the selected sample are obtained from an unbinned extended maximum likelihood fit simultaneously performed on the long and downstream K_S^0 samples. The observables used in the fit are $m_{K_S^0}$, the mass of the $K_S^0 \rightarrow \pi^+\pi^-$ candidates, $m_{\bar{D}^0}$, the mass of the $\bar{D}^0 \rightarrow K^+\pi^-$ candidates, and m_B , the mass of the B meson candidates. The probability density function (PDF) contains four terms,

$$\begin{aligned} \mathcal{P}(m_{\bar{D}^0}, m_{K_S^0}, m_B) &= \sum_{i=1}^4 N_i \mathcal{F}_i(m_{\bar{D}^0}, m_{K_S^0}, m_B) \\ &= \sum_{i=1}^4 N_i \mathcal{P}_i(m_B) \mathcal{S}_i(m_{\bar{D}^0}, m_{K_S^0}), \quad (1) \end{aligned}$$

where N_i represents the respective yield, \mathcal{P}_i parametrizes the mass distribution of the B meson candidates and \mathcal{S}_i is the joint PDF of the candidates for its decay products. The term \mathcal{F}_1 describes correctly reconstructed \bar{D}^0 and K_S^0 candidates, \mathcal{F}_2 a correctly reconstructed \bar{D}^0 meson in association with two random pions, \mathcal{F}_3 a correctly reconstructed K_S^0 meson in association with a random kaon and pion, and \mathcal{F}_4 random combinations of the four final-state particles. Johnson SU distributions [30], characterized by asymmetric tails to account for radiative losses and vertex reconstruction uncertainties, are used to parametrize the \bar{D}^0 and K_S^0 signals in $\mathcal{S}_{1,2,3}$, and exponential functions describe the backgrounds in $\mathcal{S}_{2,3,4}$.

The B mass in candidates with correctly reconstructed \bar{D}^0 and K_S^0 mesons (\mathcal{P}_1) is described by three categories of shapes: the $B_{(s)}^0 \rightarrow \bar{D}^0 K_S^0$ signal, peaking structures at lower mass from other B decays, and the combinatorial background. Signal shapes for the B^0 and B_s^0 candidates decaying to $\bar{D}^0 K_S^0$ are described by means of Johnson SU distributions with shape parameters determined from fits to the simulated signal samples, corrected for differences between the simulation and the data. The peaking structures at lower mass correspond to decays of B^0 and B_s^0 mesons that include \bar{D}^0 and K_S^0 mesons in the final state where a photon or a π meson is not reconstructed, such as $B_{(s)}^0 \rightarrow \bar{D}^{*0}(\bar{D}^0 \pi^0) K_S^0$, $B_{(s)}^0 \rightarrow \bar{D}^{*0}(\bar{D}^0 \gamma) K_S^0$, $B^+ \rightarrow \bar{D}^0 K^{*+}(K_S^0 \pi^+)$, and $B_{(s)}^0 \rightarrow \bar{D}^0 K^{*0}(K_S^0 \pi^0)$. These shapes are described with kernel estimated PDFs [31] obtained from simulation.

The same exponential function is used for the combinatorial background description of the B mass distribution in $\mathcal{P}_{1,2,3,4}$. Possible contaminations from $B_{(s)}^0 \rightarrow \bar{D}^0 \pi^+ \pi^-$ and $B_{(s)}^0 \rightarrow \bar{D}^{*0} \pi^+ \pi^-$ in \mathcal{P}_2 , and $B_{(s)}^0 \rightarrow K_S^0 K^+ \pi^-$ and

$B_{(s)}^0 \rightarrow K^{*0}(K_S^0\pi^0)K^+\pi^-$ in \mathcal{P}_3 are accounted for using the function that describes the $B_{(s)}^0$ candidates in \mathcal{P}_1 .

The PDFs \mathcal{F}_i are distinct for the long and downstream samples but share certain parameters, including those of the \bar{D}^0 signal distribution and the yield fractions of the non-combinatorial components of the B mass spectrum. Gaussian constraints are applied to the branching fraction ratios $\mathcal{B}(B_s^0 \rightarrow \bar{D}^0 K^{*0})/[\mathcal{B}(B^0 \rightarrow \bar{D}^0 K^{*0}) + \mathcal{B}(B_s^0 \rightarrow \bar{D}^0 K^{*0})]$ and $\mathcal{B}(B_{(s)}^0 \rightarrow \bar{D}^{*0}(\bar{D}^0\pi^0)K^0)/[\mathcal{B}(B_{(s)}^0 \rightarrow \bar{D}^{*0}(\bar{D}^0\gamma)K^0) + \mathcal{B}(B_{(s)}^0 \rightarrow \bar{D}^{*0}(\bar{D}^0\pi^0)K^0)]$. These constraints improve the stability of the fit and are determined from measurements of branching fractions reported in Ref. [27], corrected by the efficiencies of the relevant $B_{(s)}^0$ decays as determined from simulated samples.

Projections of the fit results on the data sample are shown in Fig. 1. The numbers of signal candidates determined

from the fit are $N(B^0 \rightarrow \bar{D}^0 K_S^0) = 219 \pm 21$, $N(B_s^0 \rightarrow \bar{D}^0 K_S^0) = 471 \pm 26$ and $N(B_s^0 \rightarrow \bar{D}^{*0} K_S^0) = 258 \pm 83$, where the uncertainties are purely statistical.

The branching fractions, \mathcal{B} , of the $B_s^0 \rightarrow \bar{D}^{(*)0} \bar{K}^0$ decays are calculated from the ratio of branching fractions between B_s^0 and B^0 ,

$$\mathcal{B}(B_s^0 \rightarrow \bar{D}^{(*)0} \bar{K}^0) = \mathcal{R}^{(*)} \times \mathcal{B}_{\text{sum}}, \quad (2)$$

where $\mathcal{B}_{\text{sum}} = \mathcal{B}(B^0 \rightarrow \bar{D}^0 K^0) + \mathcal{B}(\bar{B}^0 \rightarrow \bar{D}^0 \bar{K}^0)$ since the analysis does not distinguish between K^0 and \bar{K}^0 . The quantity

$$\mathcal{R}^{(*)} = \frac{f_d}{f_s} \frac{N(B_s^0 \rightarrow \bar{D}^{(*)0} K_S^0)}{N(B^0 \rightarrow \bar{D}^0 K_S^0) + N(\bar{B}^0 \rightarrow \bar{D}^0 K_S^0)} \frac{\epsilon_{B^0}}{\epsilon_{B_s^0}} \quad (3)$$

is the product of the production ratio of B^0 over B_s^0 decays in LHCb (f_d/f_s), the ratio of reconstructed B_s^0 and B^0

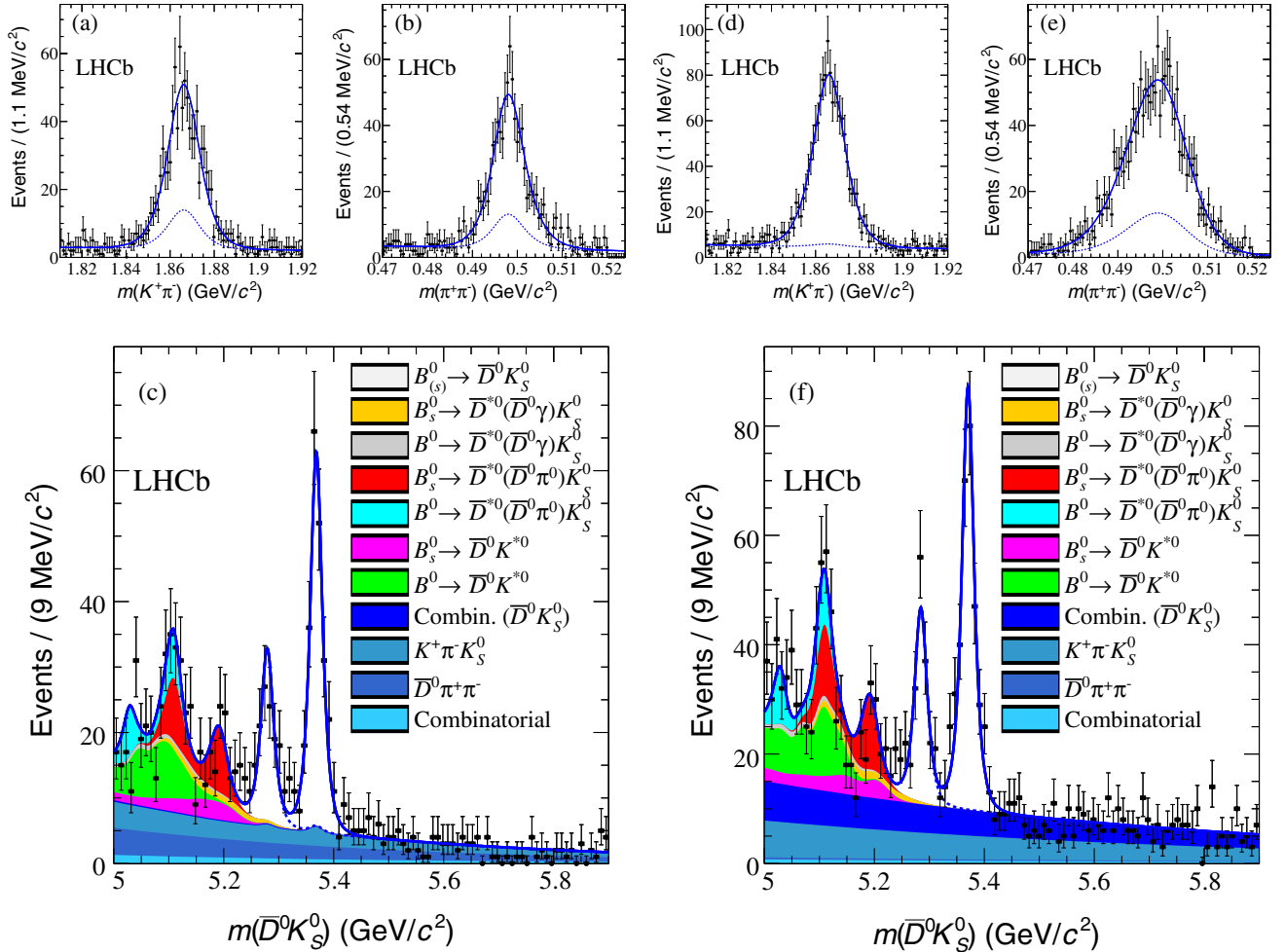


FIG. 1. The projection of the fit results (solid line) on the data sample (points) is shown for the \bar{D}^0 candidate (a),(d), the K_S^0 candidate (b),(e), and B candidate (c),(f) mass spectra. The long K_S^0 sample is shown in (a)–(c), and the downstream sample in (d)–(f). The dashed line in the \bar{D}^0 and K_S^0 candidate mass plots represents events corresponding to background categories $\mathcal{S}_{2,3,4}$ in the fit and includes peaks due to, for example, real \bar{D}^0 mesons paired with two random pions. The double-peak behavior of the $B_{(s)}^0 \rightarrow \bar{D}^{*0}(\bar{D}^0\pi^0)K_S^0$ shape is due to the missing momentum of the π^0 and the helicity amplitude of the $\bar{D}^{*0} \rightarrow \bar{D}^0\pi^0$ decay.

TABLE I. Summary of the systematic uncertainties.

Source	$B_s^0 \rightarrow \bar{D}^0 K_S^0$	$B_s^0 \rightarrow \bar{D}^{*0} K_S^0$
Fit model	5.4%	11.9%
$\epsilon_{B^0}/\epsilon_{B_s^0}$	2.4%	2.5%
f_s/f_d		5.8%
\mathcal{B}_{sum}		13.5%

signal candidates, and the ratio of efficiencies of B^0 to B_s^0 candidates decaying to $\bar{D}^{(*)0} K_S^0$ in the LHCb detector ($\epsilon_{B^0}/\epsilon_{B_s^0}$). The value of $f_s/f_d = 0.259 \pm 0.015$ is provided by previous LHCb measurements [32,33]. The ratios of efficiencies $\epsilon_{B^0 \rightarrow \bar{D}^0 K_S^0}/\epsilon_{B_s^0 \rightarrow \bar{D}^0 K_S^0} = 0.997 \pm 0.024$ and $\epsilon_{B^0 \rightarrow \bar{D}^0 K_S^0}/\epsilon_{B_s^0 \rightarrow \bar{D}^{*0} K_S^0} = 1.181 \pm 0.029$ are obtained from simulated samples. The ratio of B_s^0 and B^0 signal candidates is a free parameter in the fit and is measured to be $N(B_s^0 \rightarrow \bar{D}^0 K_S^0)/[N(B^0 \rightarrow \bar{D}^0 K_S^0) + N(\bar{B}^0 \rightarrow \bar{D}^0 K_S^0)] = 2.15 \pm 0.23$. Similarly, the ratio $N(B_s^0 \rightarrow \bar{D}^{*0} K_S^0)/[N(B^0 \rightarrow \bar{D}^0 K_S^0) + N(\bar{B}^0 \rightarrow \bar{D}^0 K_S^0)] = 1.17 \pm 0.44$ is measured.

Various sources of systematic uncertainty have been considered. These are summarized in Table I and discussed below.

The uncertainty associated with the fit model is assessed by the use of other functions for the PDFs \mathcal{P}_i and \mathcal{S}_i . For the mass distribution of the signal events, four alternative models are used. Each pseudoexperiment generated in this way is then fitted with the baseline model, and the difference of the signal yields ratio with respect to the generated value is considered. The mean of the distribution that shows the largest deviation from zero is taken as the systematic uncertainty, corresponding to 5.4% (11.9%) for $B_s^0 \rightarrow \bar{D}^0 K_S^0$ ($B_s^0 \rightarrow \bar{D}^{*0} K_S^0$).

The ratio of efficiencies of the B^0 and B_s^0 decays is determined from simulation and is limited by the finite size of the sample. The statistical uncertainties on the efficiency ratios and the statistical uncertainties of the external inputs, f_s/f_d and the branching fraction \mathcal{B}_{sum} , are propagated to the systematic uncertainty of this measurement.

To test the stability of the result with respect to the offline selection, the measurement is repeated at different

selection cuts on the multivariate classifier. The deviations from the nominal result are consistent with statistical fluctuations and no systematic uncertainty is assigned. Possible bias due to the random removal of multiple candidates is tested by removing or keeping all of them, and no significant effect is observed.

Further cross-checks on the stability of the result are made by measuring the branching fractions independently for the long and downstream K_S^0 samples, for the two different polarities of the LHCb magnet and for different running conditions. No significant effect is observed.

Only the fit model is considered when determining the systematic uncertainty on the number of signal candidates. The statistical uncertainty on the efficiencies and on f_s/f_d are also included in the sum in quadrature to give the systematic uncertainty on the ratio of branching fractions $\mathcal{R}^{(*)}$. Finally, the uncertainty on \mathcal{B}_{sum} is also included for the measurement of the branching fraction $\mathcal{B}(B_s^0 \rightarrow \bar{D}^{(*)0} \bar{K}^0)$.

Signal yields of

$$N(B^0 \rightarrow \bar{D}^0 K_S^0) = 219 \pm 21(\text{stat}) \pm 11(\text{syst}),$$

$$N(B_s^0 \rightarrow \bar{D}^0 K_S^0) = 471 \pm 26(\text{stat}) \pm 25(\text{syst}),$$

$$N(B_s^0 \rightarrow \bar{D}^{*0} K_S^0) = 258 \pm 83(\text{stat}) \pm 30(\text{syst})$$

are found. Those results correspond to the first observation of the $B_s^0 \rightarrow \bar{D}^0 K_S^0$ decay with a significance of 13.1 standard deviations and evidence for $B_s^0 \rightarrow \bar{D}^{*0} K_S^0$ with a significance of 4.4 standard deviations, where the significances are calculated using Wilks's theorem [34].

The ratios of the branching fractions are

$$\mathcal{R} = 8.3 \pm 0.9(\text{stat}) \pm 0.5(\text{syst}) \pm 0.5(\text{frag}),$$

$$\mathcal{R}^* = 5.4 \pm 2.0(\text{stat}) \pm 0.7(\text{syst}) \pm 0.3(\text{frag}).$$

Here, the correlation coefficient between the two statistical uncertainties is 68% and that between the two systematic uncertainties is 49%. Using the branching fraction $\mathcal{B}_{\text{sum}} = (5.2 \pm 0.7) \times 10^{-5}$ [27], the values of the branching fractions are

$$\mathcal{B}(B_s^0 \rightarrow \bar{D}^0 \bar{K}^0) = [4.3 \pm 0.5(\text{stat}) \pm 0.3(\text{syst}) \pm 0.3(\text{frag}) \pm 0.6(\text{norm})] \times 10^{-4},$$

$$\mathcal{B}(B_s^0 \rightarrow \bar{D}^{*0} \bar{K}^0) = [2.8 \pm 1.0(\text{stat}) \pm 0.3(\text{syst}) \pm 0.2(\text{frag}) \pm 0.4(\text{norm})] \times 10^{-4},$$

where the last uncertainty is due to the uncertainty on \mathcal{B}_{sum} . These results are consistent with theoretical predictions from Refs. [15–17], when corrections for the difference in width between the B_s^0 mass eigenstates [35] are taken into account.

This Letter reports the first observation of $B_s^0 \rightarrow \bar{D}^0 K_S^0$ and first evidence of $B_s^0 \rightarrow \bar{D}^{*0} K_S^0$. Since the theoretical

predictions for these modes have a small uncertainty, future studies with increased statistics and additional \bar{D}^0 decay modes will give significant improvements in the determination of ϕ_s and γ .

We express our gratitude to our colleagues in the CERN accelerator departments for the excellent performance of

the LHC. We thank the technical and administrative staff at the LHCb institutes. We acknowledge support from CERN and from the national agencies: CAPES, CNPq, FAPERJ, and FINEP (Brazil); NSFC (China); CNRS/IN2P3 (France); BMBF, DFG, and MPG (Germany); INFN (Italy); FOM and NWO (Netherlands); MNiSW and NCN (Poland); MEN/IFA (Romania); MinES and FANO (Russia); MinECo (Spain); SNSF and SER (Switzerland); NASU (Ukraine); STFC (United Kingdom); and the NSF (U.S.). We acknowledge the computing resources that are provided by CERN, IN2P3 (France), KIT, and DESY (Germany), INFN (Italy), SURF (Netherlands), PIC (Spain), GridPP (United Kingdom), RRCKI and Yandex LLC (Russia), CSCS (Switzerland), IFIN-HH (Romania), CBPF (Brazil), PL-GRID (Poland), and OSC (U.S.). We are indebted to the communities behind the multiple open source software packages on which we depend. Individual groups or members have received support from AvH Foundation (Germany), EPLANET, Marie Skłodowska-Curie Actions, and ERC (European Union), Conseil Général de Haute-Savoie, Labex ENIGMASS, and OCEVU, Région Auvergne (France), RFBR and Yandex LLC (Russia), GVA, XuntaGal, and GENCAT (Spain), Herchel Smith Fund, The Royal Society, Royal Commission for the Exhibition of 1851, and the Leverhulme Trust (United Kingdom).

-
- [1] B. Aubert *et al.* (BABAR Collaboration), *Phys. Rev. Lett.* **87**, 091801 (2001).
 [2] K. Abe *et al.* (Belle Collaboration), *Phys. Rev. Lett.* **87**, 091802 (2001).
 [3] R. Aaij *et al.* (LHCb Collaboration), *Phys. Lett. B* **726**, 151 (2013).
 [4] A. J. Bevan *et al.* (Belle and BABAR Collaborations), *Eur. Phys. J. C* **74**, 3026 (2014).
 [5] M. Kobayashi and T. Maskawa, *Prog. Theor. Phys.* **49**, 652 (1973).
 [6] Y. Amhis *et al.* (Heavy Flavor Averaging Group), arXiv:1412.7515.
 [7] J. Charles *et al.*, *Phys. Rev. D* **84**, 033005 (2011).
 [8] A. J. Buras, *Proc. Sci.*, EPS-HEP2009 (2009) 024 [arXiv:0910.1032].
 [9] C.-W. Chiang, A. Datta, M. Duraisamy, D. London, M. Nagashima, and A. Szykman, *J. High Energy Phys.* **04** (2010) 031.
 [10] Unless otherwise specified, the inclusion of charge conjugate reactions is implied.

- [11] M. Gronau, Y. Grossman, N. Shuhmaher, A. Soffer, and J. Zupan, *Phys. Rev. D* **69**, 113003 (2004).
 [12] R. Aaij *et al.* (LHCb Collaboration), *Phys. Lett. B* **727**, 403 (2013).
 [13] R. Fleischer, *Phys. Lett. B* **562**, 234 (2003).
 [14] B. Aubert *et al.* (BABAR Collaboration), *Phys. Rev. D* **74**, 031101 (2006).
 [15] P. Colangelo and R. Ferrandes, *Phys. Lett. B* **627**, 77 (2005).
 [16] C.-K. Chua and W.-S. Hou, *Phys. Rev. D* **77**, 116001 (2008).
 [17] C.-W. Chiang and E. Senaha, *Phys. Rev. D* **75**, 074021 (2007).
 [18] A. A. Alves, Jr. *et al.* (LHCb Collaboration), *J. Instrum.* **3**, S08005 (2008).
 [19] R. Aaij *et al.* (LHCb Collaboration), *Int. J. Mod. Phys. A* **30**, 1530022 (2015).
 [20] T. Sjöstrand, S. Mrenna, and P. Skands, *J. High Energy Phys.* **05** (2006) 026; *Comput. Phys. Commun.* **178**, 852 (2008).
 [21] I. Belyaev *et al.*, *J. Phys. Conf. Ser.* **331**, 032047 (2011).
 [22] D. J. Lange, *Nucl. Instrum. Methods Phys. Res., Sect. A* **462**, 152 (2001).
 [23] P. Golonka and Z. Was, *Eur. Phys. J. C* **45**, 97 (2006).
 [24] J. Allison, K. Amako, J. Apostolakis, H. Araujo, P. Dubois *et al.* (GEANT4 Collaboration), *IEEE Trans. Nucl. Sci.* **53**, 270 (2006); S. Agostinelli *et al.* (GEANT4 Collaboration), *Nucl. Instrum. Methods Phys. Res., Sect. A* **506**, 250 (2003).
 [25] M. Clemencic, G. Corti, S. Easo, C. R. Jones, S. Miglioranzi, M. Pappagallo, and P. Robbe, *J. Phys. Conf. Ser.* **331**, 032023 (2011).
 [26] V. V. Gligorov and M. Williams, *J. Instrum.* **8**, P02013 (2013).
 [27] K. A. Olive *et al.* (Particle Data Group), *Chin. Phys. C* **38**, 090001 (2014).
 [28] L. Breiman, J. H. Friedman, R. A. Olshen, and C. J. Stone, *Classification and Regression Trees* (Wadsworth International Group, Belmont, CA, 1984).
 [29] R. E. Schapire and Y. Freund, *J. Comput. Syst. Sci.* **55**, 119 (1997).
 [30] N. L. Johnson, *Biometrika* **36**, 149 (1949).
 [31] K. S. Cranmer, *Comput. Phys. Commun.* **136**, 198 (2001).
 [32] R. Aaij *et al.* (LHCb Collaboration), *J. High Energy Phys.* **04** (2013) 001.
 [33] LHCb Collaboration, Report No. LHCb-CONF-2013-011, 2013.
 [34] S. S. Wilks, *Ann. Math. Stat.* **9**, 60 (1938).
 [35] K. De Bruyn, R. Fleischer, R. Knegjens, P. Koppenburg, M. Merk, and N. Tuning, *Phys. Rev. D* **86**, 014027 (2012).

R. Aaij,³⁹ C. Abellán Beteta,⁴¹ B. Adeva,³⁸ M. Adinolfi,⁴⁷ A. Affolder,⁵³ Z. Ajaltouni,⁵ S. Akar,⁶ J. Albrecht,¹⁰ F. Alessio,³⁹ M. Alexander,⁵² S. Ali,⁴² G. Alkhazov,³¹ P. Alvarez Cartelle,⁵⁴ A. A. Alves Jr.,⁵⁸ S. Amato,² S. Amerio,²³ Y. Amhis,⁷ L. An,^{3,40} L. Anderlini,¹⁸ G. Andreassi,⁴⁰ M. Andreotti,^{17,b} J. E. Andrews,⁵⁹ R. B. Appleby,⁵⁵ O. Aquines Gutierrez,¹¹ F. Archilli,³⁹ P. d'Argent,¹² A. Artamonov,³⁶ M. Artuso,⁶⁰ E. Aslanides,⁶ G. Auremma,^{26,c} M. Baalouch,⁵ S. Bachmann,¹²

J. J. Back,⁴⁹ A. Badalov,³⁷ C. Baesso,⁶¹ W. Baldini,^{17,39} R. J. Barlow,⁵⁵ C. Barschel,³⁹ S. Barsuk,⁷ W. Barter,³⁹ V. Batozskaya,²⁹ V. Battista,⁴⁰ A. Bay,⁴⁰ L. Beaucourt,⁴ J. Beddow,⁵² F. Bedeschi,²⁴ I. Bediaga,¹ L. J. Bel,⁴² V. Bellee,⁴⁰ N. Belloli,^{21,d} I. Belyaev,³² E. Ben-Haim,⁸ G. Bencivenni,¹⁹ S. Benson,³⁹ J. Benton,⁴⁷ A. Berezhnoy,³³ R. Bernet,⁴¹ A. Bertolin,²³ M.-O. Bettler,³⁹ M. van Beuzekom,⁴² S. Bifani,⁴⁶ P. Billoir,⁸ T. Bird,⁵⁵ A. Birnkraut,¹⁰ A. Bizzeti,^{18,e} T. Blake,⁴⁹ F. Blanc,⁴⁰ J. Blouw,¹¹ S. Blusk,⁶⁰ V. Bocci,²⁶ A. Bondar,³⁵ N. Bondar,^{31,39} W. Bonivento,¹⁶ S. Borghi,⁵⁵ M. Borisyak,⁶⁶ M. Borsato,³⁸ T. J. V. Bowcock,⁵³ E. Bowen,⁴¹ C. Bozzi,^{17,39} S. Braun,¹² M. Britsch,¹² T. Britton,⁶⁰ J. Brodzicka,⁵⁵ N. H. Brook,⁴⁷ E. Buchanan,⁴⁷ C. Burr,⁵⁵ A. Bursche,⁴¹ J. Buytaert,³⁹ S. Cadeddu,¹⁶ R. Calabrese,^{17,b} M. Calvi,^{21,d} M. Calvo Gomez,^{37,f} P. Campana,¹⁹ D. Campora Perez,³⁹ L. Capriotti,⁵⁵ A. Carbone,^{15,g} G. Carboni,^{25,h} R. Cardinale,^{20,i} A. Cardini,¹⁶ P. Carniti,^{21,d} L. Carson,⁵¹ K. Carvalho Akiba,² G. Casse,⁵³ L. Cassina,^{21,d} L. Castillo Garcia,⁴⁰ M. Cattaneo,³⁹ Ch. Cauet,¹⁰ G. Cavallero,²⁰ R. Cenci,^{24,j} M. Charles,⁸ Ph. Charpentier,³⁹ G. Chatzikonstantinidis,⁴⁶ M. Chefdeville,⁴ S. Chen,⁵⁵ S.-F. Cheung,⁵⁶ N. Chiapolini,⁴¹ M. Chrzasczcz,^{41,27} X. Cid Vidal,³⁹ G. Ciezarek,⁴² P. E. L. Clarke,⁵¹ M. Clemencic,³⁹ H. V. Cliff,⁴⁸ J. Closier,³⁹ V. Coco,³⁹ J. Cogan,⁶ E. Cogneras,⁵ V. Cogoni,^{16,k} L. Cojocariu,³⁰ G. Collazuol,^{23,l} P. Collins,³⁹ A. Comerma-Montells,¹² A. Contu,³⁹ A. Cook,⁴⁷ M. Coombes,⁴⁷ S. Coquereau,⁸ G. Corti,³⁹ M. Corvo,^{17,b} B. Couturier,³⁹ G. A. Cowan,⁵¹ D. C. Craik,⁵¹ A. Crocombe,⁴⁹ M. Cruz Torres,⁶¹ S. Cunliffe,⁵⁴ R. Currie,⁵⁴ C. D'Ambrosio,³⁹ E. Dall'Occo,⁴² J. Dalseno,⁴⁷ P. N. Y. David,⁴² A. Davis,⁵⁸ O. De Aguiar Francisco,² K. De Bruyn,⁶ S. De Capua,⁵⁵ M. De Cian,¹² J. M. De Miranda,¹ L. De Paula,² P. De Simone,¹⁹ C.-T. Dean,⁵² D. Decamp,⁴ M. Deckenhoff,¹⁰ L. Del Buono,⁸ N. Déleage,⁴ M. Demmer,¹⁰ D. Derkach,⁶⁶ O. Deschamps,⁵ F. Dettori,³⁹ B. Dey,²² A. Di Canto,³⁹ F. Di Ruscio,²⁵ H. Dijkstra,³⁹ S. Donleavy,⁵³ F. Dordei,³⁹ M. Dorigo,⁴⁰ A. Dosil Suárez,³⁸ A. Dovbnya,⁴⁴ K. Dreimanis,⁵³ L. Dufour,⁴² G. Dujany,⁵⁵ K. Dungs,³⁹ P. Durante,³⁹ R. Dzhelezhyan,³⁶ A. Dziurda,²⁷ A. Dzyuba,³¹ S. Easo,^{50,39} U. Egede,⁵⁴ V. Egorychev,³² S. Eidelman,³⁵ S. Eisenhardt,⁵¹ U. Eitschberger,¹⁰ R. Ekelhof,¹⁰ L. Eklund,⁵² I. El Rifai,⁵ Ch. Elsassner,⁴¹ S. Ely,⁶⁰ S. Esen,¹² H. M. Evans,⁴⁸ T. Evans,⁵⁶ A. Falabella,¹⁵ C. Färber,³⁹ N. Farley,⁴⁶ S. Farry,⁵³ R. Fay,⁵³ D. Ferguson,⁵¹ V. Fernandez Albor,³⁸ F. Ferrari,¹⁵ F. Ferreira Rodrigues,¹ M. Ferro-Luzzi,³⁹ S. Filippov,³⁴ M. Fiore,^{17,39,b} M. Fiorini,^{17,b} M. Firlej,²⁸ C. Fitzpatrick,⁴⁰ T. Fiutowski,²⁸ F. Fleuret,^{7,m} K. Fohl,³⁹ P. Fol,⁵⁴ M. Fontana,¹⁶ F. Fontanelli,^{20,i} D. C. Forshaw,⁶⁰ R. Forty,³⁹ M. Frank,³⁹ C. Frei,³⁹ M. Frosini,¹⁸ J. Fu,²² E. Furfaro,^{25,h} A. Gallas Torreira,³⁸ D. Galli,^{15,g} S. Gallorini,²³ S. Gambetta,⁵¹ M. Gandelman,² P. Gandini,⁵⁶ Y. Gao,³ J. García Pardiñas,³⁸ J. Garra Tico,⁴⁸ L. Garrido,³⁷ D. Gascon,³⁷ C. Gaspar,³⁹ R. Gauld,⁵⁶ L. Gavardi,¹⁰ G. Gazzoni,⁵ D. Gerick,¹² E. Gersabeck,¹² M. Gersabeck,⁵⁵ T. Gershon,⁴⁹ Ph. Ghez,⁴ S. Gianì,⁴⁰ V. Gibson,⁴⁸ O. G. Girard,⁴⁰ L. Giubega,³⁰ V. V. Gligorov,³⁹ C. Göbel,⁶¹ D. Golubkov,³² A. Golutvin,^{54,39} A. Gomes,^{1,n} C. Gotti,^{21,d} M. Grabalosa Gándara,⁵ R. Graciani Diaz,³⁷ L. A. Granado Cardoso,³⁹ E. Graugés,³⁷ E. Graverini,⁴¹ G. Graziani,¹⁸ A. Grecu,³⁰ E. Greening,⁵⁶ P. Griffith,⁴⁶ L. Grillo,¹² O. Grünberg,⁶⁴ B. Gui,⁶⁰ E. Gushchin,³⁴ Yu. Guz,^{36,39} T. Gys,³⁹ T. Hadavizadeh,⁵⁶ C. Hadjivasiliou,⁶⁰ G. Haefeli,⁴⁰ C. Haen,³⁹ S. C. Haines,⁴⁸ S. Hall,⁵⁴ B. Hamilton,⁵⁹ X. Han,¹² S. Hansmann-Menzemer,¹² N. Harnew,⁵⁶ S. T. Harnew,⁴⁷ J. Harrison,⁵⁵ J. He,³⁹ T. Head,⁴⁰ V. Heijne,⁴² A. Heister,⁹ K. Hennessy,⁵³ P. Henrard,⁵ L. Henry,⁸ J. A. Hernando Morata,³⁸ E. van Herwijnen,³⁹ M. Heß,⁶⁴ A. Hicheur,² D. Hill,⁵⁶ M. Hoballah,⁵ C. Hombach,⁵⁵ W. Hulsbergen,⁴² T. Humair,⁵⁴ M. Hushchyn,⁶⁶ N. Hussain,⁵⁶ D. Hutchcroft,⁵³ D. Hynds,⁵² M. Idzik,²⁸ P. Ilten,⁵⁷ R. Jacobsson,³⁹ A. Jaeger,¹² J. Jalocha,⁵⁶ E. Jans,⁴² A. Jawahery,⁵⁹ M. John,⁵⁶ D. Johnson,³⁹ C. R. Jones,⁴⁸ C. Joram,³⁹ B. Jost,³⁹ N. Jurik,⁶⁰ S. Kandybei,⁴⁴ W. Kansa,⁶ M. Karacson,³⁹ T. M. Karbach,^{39,a} S. Karodia,⁵² M. Kecke,¹² M. Kelsey,⁶⁰ I. R. Kenyon,⁴⁶ M. Kenzie,³⁹ T. Ketel,⁴³ E. Khairullin,⁶⁶ B. Khanji,^{21,39,d} C. Khurewathanakul,⁴⁰ T. Kim,⁹ S. Klaver,⁵⁵ K. Klimaszewski,²⁹ O. Kochebina,⁷ M. Kolpin,¹² I. Komarov,⁴⁰ R. F. Koopman,⁴³ P. Koppenburg,^{42,39} M. Kozeiha,⁵ L. Kravchuk,³⁴ K. Kreplin,¹² M. Kreps,⁴⁹ P. Krokovny,³⁵ F. Kruse,¹⁰ W. Krzemien,²⁹ W. Kucewicz,^{27,o} M. Kucharczyk,²⁷ V. Kudryavtsev,³⁵ A. K. Kuonen,⁴⁰ K. Kurek,²⁹ T. Kvaratskheliya,³² D. Lacarrere,³⁹ G. Lafferty,^{55,39} A. Lai,¹⁶ D. Lambert,⁵¹ G. Lanfranchi,¹⁹ C. Langenbruch,⁴⁹ B. Langhans,³⁹ T. Latham,⁴⁹ C. Lazzeroni,⁴⁶ R. Le Gac,⁶ J. van Leerdam,⁴² J.-P. Lees,⁴ R. Lefèvre,⁵ A. Leflat,^{33,39} J. Lefrançois,⁷ E. Lemos Cid,³⁸ O. Leroy,⁶ T. Lesiak,²⁷ B. Leverington,¹² Y. Li,⁷ T. Likhomanenko,^{66,65} M. Liles,⁵³ R. Lindner,³⁹ C. Linn,³⁹ F. Lionetto,⁴¹ B. Liu,¹⁶ X. Liu,³ D. Loh,⁴⁹ I. Longstaff,⁵² J. H. Lopes,² D. Lucchesi,^{23,1} M. Lucio Martinez,³⁸ H. Luo,⁵¹ A. Lupato,²³ E. Luppi,^{17,b} O. Lupton,⁵⁶ N. Lusardi,²² A. Lusiani,²⁴ F. Machefert,⁷ F. Maciuc,³⁰ O. Maev,³¹ K. Maguire,⁵⁵ S. Malde,⁵⁶ A. Malinin,⁶⁵ G. Manca,⁷ G. Mancinelli,⁶ P. Manning,⁶⁰ A. Mapelli,³⁹ J. Maratas,⁵ J. F. Marchand,⁴ U. Marconi,¹⁵ C. Marin Benito,³⁷ P. Marino,^{24,39,j} J. Marks,¹² G. Martellotti,²⁶ M. Martin,⁶ M. Martinelli,⁴⁰ D. Martinez Santos,³⁸ F. Martinez Vidal,⁶⁷ D. Martins Tostes,² L. M. Massacrier,⁷ A. Massafferri,¹ R. Matev,³⁹ A. Mathad,⁴⁹ Z. Mathe,³⁹ C. Matteuzzi,²¹ A. Mauri,⁴¹ B. Maurin,⁴⁰ A. Mazurov,⁴⁶ M. McCann,⁵⁴ J. McCarthy,⁴⁶ A. McNab,⁵⁵ R. McNulty,¹³ B. Meadows,⁵⁸ F. Meier,¹⁰

M. Meissner,¹² D. Melnychuk,²⁹ M. Merk,⁴² E. Michielin,²³ D. A. Milanese,⁶³ M.-N. Minard,⁴ D. S. Mitzel,¹² J. Molina Rodriguez,⁶¹ I. A. Monroy,⁶³ S. Monteil,⁵ M. Morandin,²³ P. Morawski,²⁸ A. Mordà,⁶ M. J. Morello,^{24j} J. Moron,²⁸ A. B. Morris,⁵¹ R. Mountain,⁶⁰ F. Muheim,⁵¹ D. Müller,⁵⁵ J. Müller,¹⁰ K. Müller,⁴¹ V. Müller,¹⁰ M. Mussini,¹⁵ B. Muster,⁴⁰ P. Naik,⁴⁷ T. Nakada,⁴⁰ R. Nandakumar,⁵⁰ A. Nandi,⁵⁶ I. Nasteva,² M. Needham,⁵¹ N. Neri,²² S. Neubert,¹² N. Neufeld,³⁹ M. Neuner,¹² A. D. Nguyen,⁴⁰ T. D. Nguyen,⁴⁰ C. Nguyen-Mau,^{40,p} V. Niess,⁵ R. Niet,¹⁰ N. Nikitin,³³ T. Nikodem,¹² A. Novoselov,³⁶ D. P. O'Hanlon,⁴⁹ A. Oblakowska-Mucha,²⁸ V. Obraztsov,³⁶ S. Ogilvy,⁵² O. Okhrimenko,⁴⁵ R. Oldeman,^{16,48,k} C. J. G. Onderwater,⁶⁸ B. Osorio Rodrigues,¹ J. M. Otalora Goicochea,² A. Otto,³⁹ P. Owen,⁵⁴ A. Oyangueren,⁶⁷ A. Palano,^{14,q} F. Palombo,^{22,r} M. Palutan,¹⁹ J. Panman,³⁹ A. Papanestis,⁵⁰ M. Pappagallo,⁵² L. L. Pappalardo,^{17,b} C. Pappenheimer,⁵⁸ W. Parker,⁵⁹ C. Parkes,⁵⁵ G. Passaleva,¹⁸ G. D. Patel,⁵³ M. Patel,⁵⁴ C. Patrignani,^{20,i} A. Pearce,^{55,50} A. Pellegrino,⁴² G. Penso,^{26,s} M. Pepe Altarelli,³⁹ S. Perazzini,^{15,g} P. Perret,⁵ L. Pescatore,⁴⁶ K. Petridis,⁴⁷ A. Petrolini,^{20,i} M. Petruzzo,²² E. Picatoste Olloqui,³⁷ B. Pietrzyk,⁴ M. Piekies,²⁷ D. Pinci,²⁶ A. Pistone,²⁰ A. Piucci,¹² S. Playfer,⁵¹ M. Plo Casasus,³⁸ T. Poikela,³⁹ F. Polci,⁸ A. Poluektov,^{49,35} I. Polyakov,³² E. Polycarpo,² A. Popov,³⁶ D. Popov,^{11,39} B. Popovici,³⁰ C. Potterat,² E. Price,⁴⁷ J. D. Price,⁵³ J. Prisciandaro,³⁸ A. Pritchard,⁵³ C. Prouve,⁴⁷ V. Pugatch,⁴⁵ A. Puig Navarro,⁴⁰ G. Punzi,^{24,t} W. Qian,⁴ R. Quagliani,^{7,47} B. Rachwal,²⁷ J. H. Rademacker,⁴⁷ M. Rama,²⁴ M. Ramos Pernas,³⁸ M. S. Rangel,² I. Raniuk,⁴⁴ N. Rauschmayr,³⁹ G. Raven,⁴³ F. Redi,⁵⁴ S. Reichert,⁵⁵ A. C. dos Reis,¹ V. Renaudin,⁷ S. Ricciardi,⁵⁰ S. Richards,⁴⁷ M. Rihl,³⁹ K. Rinnert,^{53,39} V. Rives Molina,³⁷ P. Robbe,^{7,39} A. B. Rodrigues,¹ E. Rodrigues,⁵⁵ J. A. Rodriguez Lopez,⁶³ P. Rodriguez Perez,⁵⁵ S. Roiser,³⁹ V. Romanovsky,³⁶ A. Romero Vidal,³⁸ J. W. Ronayne,¹³ M. Rotondo,²³ T. Ruf,³⁹ P. Ruiz Valls,⁶⁷ J. J. Saborido Silva,³⁸ N. Sagidova,³¹ B. Saitta,^{16,k} V. Salustino Guimaraes,² C. Sanchez Mayordomo,⁶⁷ B. Sanmartin Sedes,³⁸ R. Santacesaria,²⁶ C. Santamarina Rios,³⁸ M. Santimaria,¹⁹ E. Santovetti,^{25,h} A. Sarti,^{19,s} C. Satriano,^{26,c} A. Satta,²⁵ D. M. Saunders,⁴⁷ D. Savrina,^{32,33} S. Schael,⁹ M. Schiller,³⁹ H. Schindler,³⁹ M. Schlupp,¹⁰ M. Schmelling,¹¹ T. Schmelzer,¹⁰ B. Schmidt,³⁹ O. Schneider,⁴⁰ A. Schopper,³⁹ M. Schubiger,⁴⁰ M.-H. Schune,⁷ R. Schwemmer,³⁹ B. Sciascia,¹⁹ A. Sciubba,^{26,s} A. Semennikov,³² N. Serra,⁴¹ J. Serrano,⁶ L. Sestini,²³ P. Seyfert,²¹ M. Shapkin,³⁶ I. Shapoval,^{17,44,b} Y. Shcheglov,³¹ T. Shears,⁵³ L. Shekhtman,³⁵ V. Shevchenko,⁶⁵ A. Shires,¹⁰ B. G. Siddi,¹⁷ R. Silva Coutinho,⁴¹ L. Silva de Oliveira,² G. Simi,^{23,t} M. Sirendi,⁴⁸ N. Skidmore,⁴⁷ T. Skwarnicki,⁶⁰ E. Smith,^{56,50} E. Smith,⁵⁴ I. T. Smith,⁵¹ J. Smith,⁴⁸ M. Smith,⁵⁵ H. Snoek,⁴² M. D. Sokoloff,^{58,39} F. J. P. Soler,⁵² F. Soomro,⁴⁰ D. Souza,⁴⁷ B. Souza De Paula,² B. Spaan,¹⁰ P. Spradlin,⁵² S. Sridharan,³⁹ F. Stagni,³⁹ M. Stahl,¹² S. Stahl,³⁹ S. Stefkova,⁵⁴ O. Steinkamp,⁴¹ O. Stenyakin,³⁶ S. Stevenson,⁵⁶ S. Stoica,³⁰ S. Stone,⁶⁰ B. Storaci,⁴³ S. Stracka,^{24,j} M. Straticiu,³⁰ U. Straumann,⁴¹ L. Sun,⁵⁸ W. Sutcliffe,⁵⁴ K. Swientek,²⁸ S. Swientek,¹⁰ V. Syropoulos,⁴³ M. Szczekowski,²⁹ T. Szumlak,²⁸ S. T'Jampens,⁴ A. Tayduganov,⁶ T. Tekampe,¹⁰ G. Tellarini,^{17,b} F. Teubert,³⁹ C. Thomas,⁵⁶ E. Thomas,³⁹ J. van Tilburg,⁴² V. Tisserand,⁴ M. Tobin,⁴⁰ J. Todd,⁵⁸ S. Tolk,⁴³ L. Tomassetti,^{17,b} D. Tonelli,³⁹ S. Topp-Joergensen,⁵⁶ N. Torr,⁵⁶ E. Tournefier,⁴ S. Tourneur,⁴⁰ K. Trabelsi,⁴⁰ M. Traill,⁵² M. T. Tran,⁴⁰ M. Tresch,⁴¹ A. Trisovic,³⁹ A. Tsaregorodtsev,⁶ P. Tsopelas,⁴² N. Tuning,^{42,39} A. Ukleja,²⁹ A. Ustyuzhanin,^{66,65} U. Uwer,¹² C. Vacca,^{16,39,k} V. Vagnoni,¹⁵ G. Valenti,¹⁵ A. Vallier,⁷ R. Vazquez Gomez,¹⁹ P. Vazquez Regueiro,³⁸ C. Vázquez Sierra,³⁸ S. Vecchi,¹⁷ M. van Veghel,⁴² J. J. Velthuis,⁴⁷ M. Veltri,^{18,u} G. Veneziano,⁴⁰ M. Vesterinen,¹² B. Viaud,⁷ D. Vieira,² M. Vieites Diaz,³⁸ X. Vilasis-Cardona,^{37,f} V. Volkov,³³ A. Vollhardt,⁴¹ D. Voong,⁴⁷ A. Vorobyev,³¹ V. Vorobyev,³⁵ C. Voß,⁶⁴ J. A. de Vries,⁴² R. Waldi,⁶⁴ C. Wallace,⁴⁹ R. Wallace,¹³ J. Walsh,²⁴ J. Wang,⁶⁰ D. R. Ward,⁴⁸ N. K. Watson,⁴⁶ D. Websdale,⁵⁴ A. Weiden,⁴¹ M. Whitehead,³⁹ J. Wicht,⁴⁹ G. Wilkinson,^{56,39} M. Wilkinson,⁶⁰ M. Williams,³⁹ M. P. Williams,⁴⁶ M. Williams,⁵⁷ T. Williams,⁴⁶ F. F. Wilson,⁵⁰ J. Wimberley,⁵⁹ J. Wishahi,¹⁰ W. Wislicki,²⁹ M. Witek,²⁷ G. Wormser,⁷ S. A. Wotton,⁴⁸ K. Wraight,⁵² S. Wright,⁴⁸ K. Wyllie,³⁹ Y. Xie,⁶² Z. Xu,⁴⁰ Z. Yang,³ J. Yu,⁶² X. Yuan,³⁵ O. Yushchenko,³⁶ M. Zangoli,¹⁵ M. Zavertyaev,^{11,v} L. Zhang,³ Y. Zhang,³ A. Zhelezov,¹² A. Zhokhov,³² L. Zhong,³ V. Zhukov,⁹ and S. Zucchelli¹⁵

(LHCb Collaboration)

¹Centro Brasileiro de Pesquisas Físicas (CBPF), Rio de Janeiro, Brazil²Universidade Federal do Rio de Janeiro (UFRJ), Rio de Janeiro, Brazil³Center for High Energy Physics, Tsinghua University, Beijing, China⁴LAPP, Université Savoie Mont-Blanc, CNRS/IN2P3, Annecy-Le-Vieux, France⁵Clermont Université, Université Blaise Pascal, CNRS/IN2P3, LPC, Clermont-Ferrand, France⁶CPPM, Aix-Marseille Université, CNRS/IN2P3, Marseille, France⁷LAL, Université Paris-Sud, CNRS/IN2P3, Orsay, France⁸LPNHE, Université Pierre et Marie Curie, Université Paris Diderot, CNRS/IN2P3, Paris, France

- ⁹*I. Physikalisches Institut, RWTH Aachen University, Aachen, Germany*
- ¹⁰*Fakultät Physik, Technische Universität Dortmund, Dortmund, Germany*
- ¹¹*Max-Planck-Institut für Kernphysik (MPIK), Heidelberg, Germany*
- ¹²*Physikalisches Institut, Ruprecht-Karls-Universität Heidelberg, Heidelberg, Germany*
- ¹³*School of Physics, University College Dublin, Dublin, Ireland*
- ¹⁴*Sezione INFN di Bari, Bari, Italy*
- ¹⁵*Sezione INFN di Bologna, Bologna, Italy*
- ¹⁶*Sezione INFN di Cagliari, Cagliari, Italy*
- ¹⁷*Sezione INFN di Ferrara, Ferrara, Italy*
- ¹⁸*Sezione INFN di Firenze, Firenze, Italy*
- ¹⁹*Laboratori Nazionali dell'INFN di Frascati, Frascati, Italy*
- ²⁰*Sezione INFN di Genova, Genova, Italy*
- ²¹*Sezione INFN di Milano Bicocca, Milano, Italy*
- ²²*Sezione INFN di Milano, Milano, Italy*
- ²³*Sezione INFN di Padova, Padova, Italy*
- ²⁴*Sezione INFN di Pisa, Pisa, Italy*
- ²⁵*Sezione INFN di Roma Tor Vergata, Roma, Italy*
- ²⁶*Sezione INFN di Roma La Sapienza, Roma, Italy*
- ²⁷*Henryk Niewodniczanski Institute of Nuclear Physics Polish Academy of Sciences, Kraków, Poland*
- ²⁸*AGH—University of Science and Technology, Faculty of Physics and Applied Computer Science, Kraków, Poland*
- ²⁹*National Center for Nuclear Research (NCBJ), Warsaw, Poland*
- ³⁰*Horia Hulubei National Institute of Physics and Nuclear Engineering, Bucharest-Magurele, Romania*
- ³¹*Petersburg Nuclear Physics Institute (PNPI), Gatchina, Russia*
- ³²*Institute of Theoretical and Experimental Physics (ITEP), Moscow, Russia*
- ³³*Institute of Nuclear Physics, Moscow State University (SINP MSU), Moscow, Russia*
- ³⁴*Institute for Nuclear Research of the Russian Academy of Sciences (INR RAN), Moscow, Russia*
- ³⁵*Budker Institute of Nuclear Physics (SB RAS) and Novosibirsk State University, Novosibirsk, Russia*
- ³⁶*Institute for High Energy Physics (IHEP), Protvino, Russia*
- ³⁷*Universitat de Barcelona, Barcelona, Spain*
- ³⁸*Universidad de Santiago de Compostela, Santiago de Compostela, Spain*
- ³⁹*European Organization for Nuclear Research (CERN), Geneva, Switzerland*
- ⁴⁰*Ecole Polytechnique Fédérale de Lausanne (EPFL), Lausanne, Switzerland*
- ⁴¹*Physik-Institut, Universität Zürich, Zürich, Switzerland*
- ⁴²*Nikhef National Institute for Subatomic Physics, Amsterdam, The Netherlands*
- ⁴³*Nikhef National Institute for Subatomic Physics and VU University Amsterdam, Amsterdam, The Netherlands*
- ⁴⁴*NSC Kharkiv Institute of Physics and Technology (NSC KIPT), Kharkiv, Ukraine*
- ⁴⁵*Institute for Nuclear Research of the National Academy of Sciences (KINR), Kyiv, Ukraine*
- ⁴⁶*University of Birmingham, Birmingham, United Kingdom*
- ⁴⁷*H.H. Wills Physics Laboratory, University of Bristol, Bristol, United Kingdom*
- ⁴⁸*Cavendish Laboratory, University of Cambridge, Cambridge, United Kingdom*
- ⁴⁹*Department of Physics, University of Warwick, Coventry, United Kingdom*
- ⁵⁰*STFC Rutherford Appleton Laboratory, Didcot, United Kingdom*
- ⁵¹*School of Physics and Astronomy, University of Edinburgh, Edinburgh, United Kingdom*
- ⁵²*School of Physics and Astronomy, University of Glasgow, Glasgow, United Kingdom*
- ⁵³*Oliver Lodge Laboratory, University of Liverpool, Liverpool, United Kingdom*
- ⁵⁴*Imperial College London, London, United Kingdom*
- ⁵⁵*School of Physics and Astronomy, University of Manchester, Manchester, United Kingdom*
- ⁵⁶*Department of Physics, University of Oxford, Oxford, United Kingdom*
- ⁵⁷*Massachusetts Institute of Technology, Cambridge, Massachusetts, USA*
- ⁵⁸*University of Cincinnati, Cincinnati, Ohio, USA States*
- ⁵⁹*University of Maryland, College Park, Maryland, USA*
- ⁶⁰*Syracuse University, Syracuse, New York, USA*
- ⁶¹*Pontifícia Universidade Católica do Rio de Janeiro (PUC-Rio), Rio de Janeiro, Brazil
(associated with Institution Universidade Federal do Rio de Janeiro (UFRJ), Rio de Janeiro, Brazil)*
- ⁶²*Institute of Particle Physics, Central China Normal University, Wuhan, Hubei, China
(associated with Institution Center for High Energy Physics, Tsinghua University, Beijing, China)*
- ⁶³*Departamento de Física, Universidad Nacional de Colombia, Bogota, Colombia
(associated with Institution LPNHE, Université Pierre et Marie Curie, Université Paris Diderot, CNRS/IN2P3, Paris, France)*
- ⁶⁴*Institut für Physik, Universität Rostock, Rostock, Germany
(associated with Institution Physikalisches Institut, Ruprecht-Karls-Universität Heidelberg, Heidelberg, Germany)*

⁶⁵*National Research Centre Kurchatov Institute, Moscow, Russia*

(associated with Institution Institute of Theoretical and Experimental Physics (ITEP), Moscow, Russia)

⁶⁶*Yandex School of Data Analysis, Moscow, Russia*

(associated with Institution Institute of Theoretical and Experimental Physics (ITEP), Moscow, Russia)

⁶⁷*Instituto de Fisica Corpuscular (IFIC), Universitat de Valencia-CSIC, Valencia, Spain*

(associated with Institution Universitat de Barcelona, Barcelona, Spain)

⁶⁸*Van Swinderen Institute, University of Groningen, Groningen, The Netherlands*

(associated with Institution Nikhef National Institute for Subatomic Physics, Amsterdam, The Netherlands)

^aDeceased.

^bAlso at Università di Ferrara, Ferrara, Italy.

^cAlso at Università della Basilicata, Potenza, Italy.

^dAlso at Università di Milano Bicocca, Milano, Italy.

^eAlso at Università di Modena e Reggio Emilia, Modena, Italy.

^fAlso at LIFAELS, La Salle, Universitat Ramon Llull, Barcelona, Spain.

^gAlso at Università di Bologna, Bologna, Italy.

^hAlso at Università di Roma Tor Vergata, Roma, Italy.

ⁱAlso at Università di Genova, Genova, Italy.

^jAlso at Scuola Normale Superiore, Pisa, Italy.

^kAlso at Università di Cagliari, Cagliari, Italy.

^lAlso at Università di Padova, Padova, Italy.

^mAlso at Laboratoire Leprince-Ringuet, Palaiseau, France.

ⁿAlso at Universidade Federal do Triângulo Mineiro (UFTM), Uberaba-MG, Brazil.

^oAlso at AGH—University of Science and Technology, Faculty of Computer Science, Electronics and Telecommunications, Kraków, Poland.

^pAlso at Hanoi University of Science, Hanoi, Viet Nam.

^qAlso at Università di Bari, Bari, Italy.

^rAlso at Università degli Studi di Milano, Milano, Italy.

^sAlso at Università di Roma La Sapienza, Roma, Italy.

^tAlso at Università di Pisa, Pisa, Italy.

^uAlso at Università di Urbino, Urbino, Italy.

^vAlso at P.N. Lebedev Physical Institute, Russian Academy of Science (LPI RAS), Moscow, Russia.